The role of the C terminus of the SNARE protein SNAP-25 in fusion pore opening and a model for fusion pore mechanics

Qinghua Fang*, Khajak Berberian*, Liang-Wei Gong*†, Ismail Hafez*‡, Jakob B. Sørensen§, and Manfred Lindau*¶

*School of Applied and Engineering Physics, 212 Clark Hall, Cornell University, Ithaca, NY 14853; and §Department of Membrane Biophysics, Max Planck Institute for Biophysical Chemistry, D-37077 Göttingen, Germany

Edited by Axel T. Brunger, Stanford University, Stanford, CA, and approved September 4, 2008 (received for review June 2, 2008)

Formation of a fusion pore between a vesicle and its target membrane is thought to involve the so-called SNARE protein complex. However, there is no mechanistic model explaining how the fusion pore is opened by conformational changes in the SNARE complex. It has been suggested that C-terminal zipping triggers fusion pore opening. A SNAP-25 mutant named SNAP-25Δ9 (lacking the last nine C-terminal residues) should lead to a less-tight C-terminal zipping. Single exocytotic events in chromaffin cells expressing this mutant were characterized by carbon fiber amperometry and cell-attached patch capacitance measurements. Cells expressing SNAP-25Δ9 displayed smaller amperometric ''foot-current'' currents, reduced fusion pore conductances, and lower fusion pore expansion rates. We propose that SNARE/lipid complexes form proteolipid fusion pores. Fusion pores involving the SNAP-25Δ9 mutant will be less tightly zipped and may lead to a longer fusion pore structure, consistent with the observed decrease of fusion pore conductance.

amperometry | capacitance measurement | chromaffin cell | exocytosis | patch clamp

The formation of a fusion pore, the connection between vesicular lumen and extracellular space, is a key step of exocytosis (1, 2) that may be driven by a conformational change in the SNARE complex (3). It has been proposed that a preassembled fusion pore may initiate rapid transmitter release in neurosecretion (4), and it was suggested that the outer part of the fusion pore may be formed by a ring of ≈5 or 7 syntaxin transmembrane domains (5, 6). However, there is considerable controversy regarding the fusion pore structure, and an alternative hypothesis is that fusion pore formation occurs via a hemifusion intermediate (7, 8). Although the structure of the fusion pore remains elusive, current models place the C termini of all three SNAREs in or near the fusion pore (9).

Deletions of 4–9 aa at the C terminus of SNAP-25 reduce exocytosis in chromaffin cells (10, 11) and affect the kinetics of single release events (11), and mutations in the C-terminal part of SNAP-25 decrease the rate of exocytosis, suggesting that fusion is driven by N- to C-terminal zipping (12). Such manipulations of the SNAP-25 C terminus should lead to a less-tight zipping at the C-terminal side of the SNARE complex and may be expected to lead to fusion pores with different structure and stability. The opening of single fusion pores can be detected by carbon fiber amperometry as a "foot signal" (13) preceding an amperometric current spike that reflects the flux of catecholamines released from individual vesicles. The amperometric foot signal reflects flux of transmitter through narrow fusion pores with conductance <2 nS by electrodiffusion (14–16).

To study the role of the SNAP-25 C terminus in fusion pore formation, SNAP-25Δ9 (lacking the last nine C-terminal residues) coupled with GFP was overexpressed in bovine chromaffin cells. Single exocytotic events were characterized by measurements of amperometric foot currents (13) and cell-attached patch capacitance measurements (17–19). Cells overexpressing SNAP-25Δ9 displayed smaller amperometric foot currents, reduced fusion pore conductances, and lower fusion pore expansion rates. The results suggest a model for fusion pore mechanics that couple C-terminal zipping of the SNARE complex to the opening of a proteolipid fusion pore.

Results

Carbon fiber amperometry was applied to determine whether deletion of the C-terminal 9 aa of SNAP-25 affected transmitter release from single vesicles (Fig. 1). Exocytosis was stimulated by high K^+ depolarization. Cells overexpressing SNAP-25Δ9 showed fewer amperometric events (12.8 ± 2.0 events per cell) than cells overexpressing SNAP-25 wild-type (23.2 ± 2.3 events per cell) and noninfected control cells (28.6 ± 4.8 events per cell) (Fig. 1 *A* and *C*). The reduced number of exocytotic events is consistent with previous whole-cell patch-clamp capacitance measurement where exocytosis was stimulated by flash photolysis of caged calcium (10). To compare the amount and kinetics of transmitter release from single vesicles, each amperometric spike was characterized by its quantal size (spike charge from integrated amperometric current), amperometric spike amplitude, amperometric spike half-width, amperometric foot duration, and average foot current amplitude (Fig. 1*B*). The amount of transmitter released from a vesicle did not change in cells overexpressing SNAP-25Δ9 (Fig. 1*D*). However, the mean amperometric spike peak amplitude of SNAP-25Δ9-expressing cells (42.8 ± 6.0 pA) was significantly smaller than those of cells overexpressing SNAP-25 wild-type (62.7 ± 7.3 pA) and of control cells (78.2 ± 12.6 pA) (Fig. 1*E*). Accordingly, the mean amperometric spike half-width of SNAP-25Δ9-expressing cells was significantly increased (19.2 ± 3.4 ms) compared with control cells (9.9 ± 1.1 ms) and cells overexpressing SNAP-25 wild-type (11.2 ± 1.7 ms), indicating that SNAP-25Δ9 reduces the rate of transmitter release from individual vesicles (Fig. 1*F*). Virtually identical changes in amperometric spike kinetics were previously observed after GFP-SNAP-25Δ6 overexpression (11).

The amperometric foot current amplitude indicates the flux of molecules through the pore, and the duration of the foot signal indicates the time interval from fusion pore opening to its rapid expansion (14, 16). In cells overexpressing SNAP-25Δ9, the mean foot duration (Fig. 1*G*) was 83 ± 16 ms, significantly longer than in wild-type cells and cells overexpressing wtSNAP-25

Author contributions: M.L. designed research; Q.F., K.B., L.-W.G., and I.H. performed research; J.B.S. contributed new reagents/analytic tools; Q.F., K.B., L.-W.G., and I.H. analyzed data; and Q.F. and M.L. wrote the paper.

The authors declare no conflict of interest.

This article is a PNAS Direct Submission.

†Present address: Department of Biological Sciences, University of Illinois, Chicago, IL 60607.

‡Present address: Department of Biochemistry and Molecular Biology, University of British Columbia, Vancouver, BC, Canada V6T 1Z3.

¶To whom correspondence should be addressed. E-mail: ml95@cornell.edu.

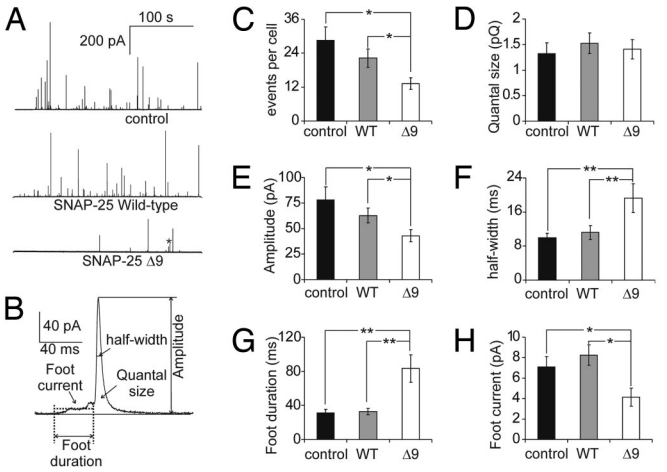

Fig. 1. Removing the nine C-terminal amino acids of SNAP-25 reduces the rate of exocytotic events and modulates the dynamics of single release events. (*A*) Amperometric recording of catecholamine release from a control bovine chromaffin cell (*Top*), a cell overexpressing wild-type SNAP-25 (*Middle*), and SNAP-25Δ9 (*Bottom*) during continuous stimulation with 100 mM KCl. (*B*) A single amperometric event from the SNAP-25Δ9 trace on expanded scale illustrating the parameters analyzed for amperometric spikes (foot duration, mean foot current, spike half-width, spike amplitude, and quantal size). (*C–H*) Statistical analysis of spike frequency (*C*), quantal size (*D*), spike amplitude (*E*), spike half-width (*F*), foot duration (*G*), and foot current (*H*) obtained for control cells (black, $n = 29$ cells, 11–121 events per cell), cells overexpressing wtSNAP-25 (gray, $n = 18$ cells, 10–67 events per cell), and cells expressing SNAP-25Δ9 (white, $n = 16$ cells, 5–30 events per cell). *, $P < 0.05$; **, $P < 0.01$ (Student's *t* test). The quantal size of amperometric events of control cells, cells overexpressing wtSNAP-25, and SNAP-25Δ9 were 1.32 ± 0.21, 1.53 ± 0.20, and 1.47 ± 0.19 pC, respectively.

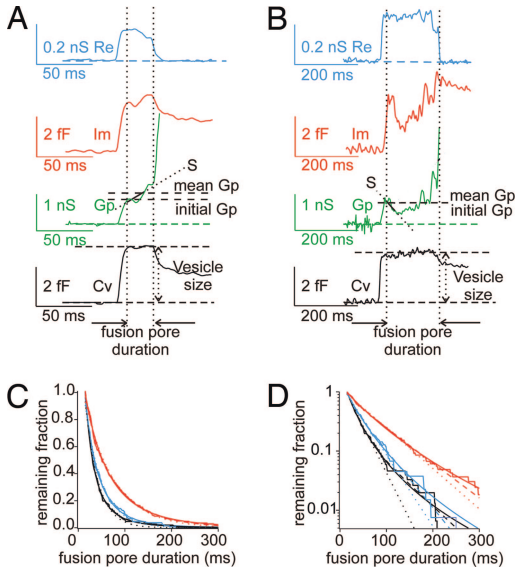

Fig. 2. Fusion pore analysis for SNAP-25Δ9-expressing cells by cell-attached capacitance measurements. (*A*) Real part (Re, blue) and imaginary part of admittance change (Im, red), fusion pore conductance (Gp, green), and vesicle capacitance (Cv, black) during a typical fusion pore opening with a monotonous Gp increase from initial fusion pore opening to rapid expansion. Fusion pore opening was characterized by quantifying initial fusion pore conductance at the time where Cv had reached its final value within a few percent, fusion pore expansion rate from slope *S* of linear regression during the first 15 ms of the fusion pore, fusion pore duration, and mean fusion pore conductance. (*B*) Re (blue), Im (red), Gp (green), and Cv (black) for a slow fusion pore opening with Gp fluctuations and negative initial slope *S*. In *A* and *B*, note that Cv is constant during the expansion of the fusion pore, but a capacitance decrease is evident after full expansion of the fusion pore. One possible explanation for this phenomenon is that in the cell-attached configuration, the full incorporation of a vesicle into the patch membrane and the resulting increase in patch area is followed by increased attachment (sealing) of part of the patch membrane to the glass, leading to a decrease in capacitance (20). (*C*) Survival curves of fusion pore duration for control cells (black, 151 events), cells overexpressing wtSNAP-25 (blue, 141 events), and cells overexpressing SNAP-25Δ9 (red, 166 events). The thinner smooth lines show fits of the decay with a single exponential (dotted line), double exponential (dashed line), and power law (solid line). (*D*) Survival curves and fits as in *C* but on a logarithmic scale.

(31 ± 4 ms and 33 ± 4 ms, respectively). The average foot current amplitude (Fig. 1*H*) was smaller (4.14 ± 0.87 pA) in SNAP-25Δ9 cells than in wild-type cells (7.10 ± 1.00 pA) and cells overexpressing wtSNAP-25 (8.26 ± 1.00 pA). These results indicate that fusion pores involving SNAP-25Δ9 have a longer lifetime and show a reduced flux of catecholamine.

The reduced flux of catecholamine through fusion pores in cells overexpressing SNAP-25Δ9 may reflect a distorted structure of the fusion pore. To test this hypothesis, we determined fusion pore conductances by cell-attached capacitance measurements (17, 19), which provide a more direct assessment of fusion pore properties. Fusion pore openings in cells overexpressing SNAP-25Δ9 show variable properties (Fig. 2), as do nontransfected bovine chromaffin cells (16). Typically (Fig. 2*A*), the fusion pore opening manifests itself as a transient increase in the real part (Re) of the patch admittance on the time scale of 5–50 ms associated with a time-resolved increase in the imaginary part (Im). From these traces, the time course of fusion pore conductance (Gp) and capacitance (Cv) were calculated. After the initial opening of the fusion pore, Gp increased rather monotonically. The initial Gp was taken at a time point where the Cv trace reached the full vesicle capacitance within <10% to account for the time resolution of the admittance measurement. The initial fusion pore expansion rate was determined as the initial slope *S* of a linear fit to the first 15 ms of the fusion pore after its initial opening (15). The lifetime of the fusion pore (duration) was taken as the time between its initial opening and the time where Gp exceeded 2 ns, which was always after the slope of Gp increased sharply, indicating rapid fusion pore expansion. As an additional characteristic parameter, we determined the mean fusion pore conductance between initial opening and rapid expansion. Some fusion pore openings were slower exhibiting Gp fluctuations, and the initial slope was occasionally negative (Fig. 2*B*). The correctness of the fusion pore conductance determination was confirmed for all analyzed events by verification of a constant Cv during fusion pore expansion. In some events (as in Fig. 2 *A* and *B*) the full fusion pore expansion was followed by a gradual capacitance decrease as previously reported for exocytosis of neutrophil granules (20). After a long fusion pore flicker, some fusion pores closed eventually in a so-called "kiss-and-run" event as reported for nontransfected chromaffin cells (14, 15, 21).

From the measured fusion pore durations, fusion pore survival curves were constructed for the three groups: wild-type cells, cells overexpressing wtSNAP-25, and cells overexpressing SNAP-25Δ9 (Fig. 2*C*), representing the cumulative fusion pore lifetime distributions. They show that the fusion pore duration is markedly increased in cells overexpressing SNAP-25Δ9 but is little affected in cells overexpressing wtSNAP-25. Single exponential fit time constants τ are given in Table 1. The single exponentials (Fig. 2*C*, dotted lines) do not represent a very good fit, however, which is clearly evident in the logarithmic graph of Fig. 2*D* (dotted lines), and the deviations suggest more than one component. Double exponential fits (Fig. 2 *C* and *D*, dashed lines) reproduce the data well. The fitted parameters (Table 1: τ-fast, τ-slow, and amplitude ratio A-slow/A-fast) show that the

Table 1. Fusion pore survival curve fit parameters obtained with single-exponential (τ), double-exponential (τ-fast, τ-slow, A-slow/A-fast) and power law (1/k, n) fits

Cell group	τ, ms	τ-Fast, ms	τ-Slow, ms	A-slow A-fast	1/k, ms	n
Control	28 ± 1	18 ± 1	60 ± 2	0.19 ± 0.02	15 ± 1	3.2 ± 0.2
SNAP-25	36 ± 1	12 ± 1	44 ± 1	0.79 ± 0.08	25 ± 1	4.5 ± 0.2
SNAP-25Δ9	64 ± 1	17 ± 2	74 ± 1	1.6 ± 0.1	48 ± 1	5.0 ± 0.3

main change in cells overexpressing SNAP-25Δ9 appears to be a marked increase in the slow component.

A double-exponential fit is based on the assumption of two distinct fusion pore populations. However, it appears more likely that fusion pores may in fact represent a larger set of various populations and could, for instance, be formed at variable Ca^{2+} concentrations (22–25), by variable synaptotagmin interactions (26, 27) or possibly by a variable number of SNARE protein complexes. A continuous distribution of rate constants leads to a time course that can be described by a power law $f(t) = A(1 + kt/n)^{-n}$, where k is the peak rate constant of the distribution, and the parameter n corresponds to the width of the distribution (28, 29). For large n, the distribution becomes very narrow, and the time course approaches single-exponential behavior. Fits with this power law (Fig. 2 *C* and *D*, smooth solid lines) reproduce the measured curves at least as well as double-exponential fits, although only three instead of four free parameters are fitted. The reciprocal peak rate constants were 15 and 25 ms for untransfected cells and cells overexpressing wtSNAP-25, respectively. The value was much larger (48 ms) for cells overexpressing SNAP-25Δ9. The parameter n was lowest for control cells, indicating that the fusion pore population is normally rather inhomogeneous. The larger n values for cells overexpressing wtSNAP-25 or SNAP-25Δ9 indicate more homogeneous fusion pore kinetics.

For a more conservative comparison of average fusion pore duration with average foot duration, we calculated the median fusion pore duration for each patch and then the mean of the median values (Fig. 3*A*), which also reveals the increase of fusion pore lifetime in cells expressing SNAP-25Δ9. For this analysis, only patches with at least five events were included. The average fusion pore durations determined in this way were not significantly different between nontransfected cells (35 ± 4 ms) and cells overexpressing wtSNAP-25 (41 ± 5 ms). They were significantly longer in cells overexpressing SNAP-25Δ9 (73 ± 12 ms), confirming the results of the survival curve fits. The values are also in very good agreement with those observed for the amperometric foot signal duration (Fig. 1*G*).

The average capacitance step sizes obtained from control cells, cells overexpressing wtSNAP-25, and SNAP-25Δ9 (Fig. 3*B*) were not significantly different, indicating that vesicle sizes were unchanged. Together with the unchanged quantal size (Fig. 1*D*), this suggests that vesicular catecholamine concentrations are also not affected. Therefore, the reduced amperometric foot current should be due to reduced permeability of the fusion pore. As for ion channels, changes in the structure of the fusion pore should be reflected in changes of its conductance. The average initial fusion pore conductance (Fig. 3*C*) was significantly lower in cells expressing SNAP-25Δ9 (236 ± 25 ps) than in nontransfected cells (330 ± 21 ps) and in cells overexpressing wtSNAP-25 (339 ± 38 ps). Also, the average fusion pore conductance between initial opening and expansion beyond 2 ns (Fig. 3*D*) was significantly reduced in SNAP-25Δ9-expressing cells (597 ± 44 ps) compared with nontransfected (761 ± 42 ps) and wtSNAP-25-overexpressing cells (758 ± 42 ps). These results indicate that the structure of the fusion pore is modified in cells expressing SNAP-25Δ9. The mean fusion pore expansion rate (Fig. 3*E*) is also markedly slower for fusion pores in cells expressing SNAP-25Δ9 (25 ± 4 ns/s) compared with cells overexpressing wtSNAP-25 (55 ± 7 ns/s) and control cells (51 ± 5 ns/s).

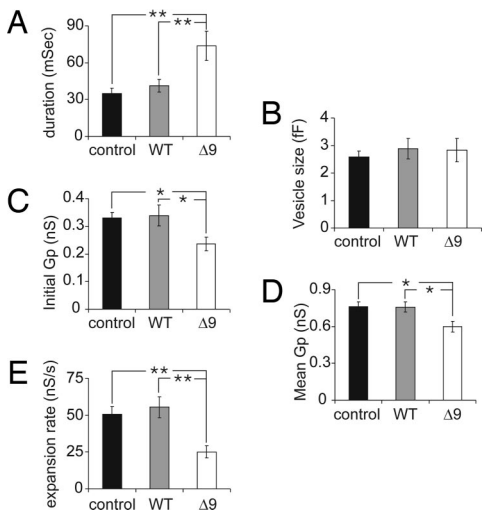

Fig. 3. Removing the nine C-terminal amino acids of SNAP-25 modifies fusion pore properties. Statistical analysis of fusion pore duration (*A*), capacitance step size (*B*), initial fusion pore conductance (*C*), mean fusion pore conductance (*D*), and fusion pore expansion rate (*E*) of control cells (black, n = 16 cells, 5–32 events per cell), cells overexpressing wtSNAP-25 (gray, n = 11 cells, 5–28 events per cell) or SNAP-25Δ9 (white, n = 11 cells, 5–21 events per cell). *, $P < 0.05$; **, $P < 0.01$ (Student's t test).

Discussion

It is still unclear how exocytotic fusion pores are formed. To achieve rapid transmitter release in neurosecretion, a preassembled fusion pore may open in response to stimulation (4). It has been proposed that the outer part of the fusion pore may be a ring of ≈5 or 7 syntaxin transmembrane domains (5, 6). However, the transmembrane domains of syntaxin as well as synaptobrevin are hydrophobic, and it is not immediately evident how they could form a pore that allows for permeation of charged transmitter molecules as well as other ions in a way similar to an ion channel (16). An alternative hypothesis is that fusion pore formation occurs via a hemifusion intermediate (7, 8). In those models, the role of SNARE proteins is to impose tension and curvature, leading to merging of lipids forming a hemifusion intermediate that ultimately breaks, forming a purely lipidic fusion pore. Although the structure of the fusion pore remains elusive, current models place the C termini of all three SNAREs in or near the fusion pore (9).

SNAP-25 is one of the essential components in the neuronal SNARE complex mediating exocytosis of synaptic vesicles as well as chromaffin granules. It has been suggested that only the N-terminal part of the SNARE complex is zipped in the primed state (Fig. 4*A*), whereas N- to C-terminal zipping and the associated conformational change in the C terminus of the SNARE complex is thought to induce fusion pore formation (12). Here, we have shown that SNARE complexes involving SNAP-25Δ9 produce fusion pores with smaller conductance,

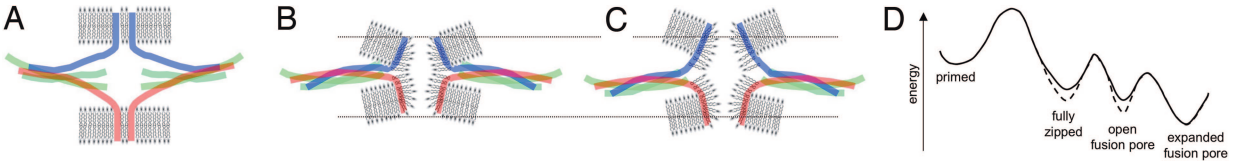

Fig. 4. Schematic model of fusion pore mechanics. (*A*) Primed state with N-terminally zipped SNARE complex. (*B*) Fully zipped SNARE complex and early fusion pore. (*C*) Less-tightly zipped SNARE complex involving the SNAP-25Δ9 mutant may produce a longer fusion pore. The horizontal lines are drawn to aid in identifying the increased fusion pore length. (*D*) Schematic energy diagram for the different states including contributions form the SNARE domain interactions as wells as the transmembrane domains and membrane interactions.

longer fusion pore duration, and slower expansion rate. Although the C terminus of SNAP-25 is unlikely to protrude directly into the fusion pore, the reduced conductance of the fusion pore and the associated reduced flux of catecholamines suggest a change in fusion pore structure. This may be a decrease in fusion pore diameter, an increase in fusion pore length, or an even more complex structural change.

Fig. 4*B* shows a SNARE complex structure that is based on the structure of the fully zipped four-helix bundle as observed by x-ray crystallography (9). The coiled coil extends almost directly to the transmembrane domains of synaptobrevin and syntaxin such that, in this state, the vesicle and plasma membrane are pulled very close together. This fully zipped state is thought to lead to fusion pore opening. Synaptic vesicles have a very high protein content in their membrane, and it has been suggested that the majority of lipid molecules may be in direct contact with membrane proteins (30). It thus appears that there will be very few "free" lipid molecules, suggesting that a lipidic hemifusion state may be unlikely because of the lack of sufficiently sized lipid areas. Because the transmembrane domains of synaptobrevin and syntaxin are hydrophobic, we propose a proteolipidic fusion pore (Fig. 4*B*), where the conformational change in the SNARE complex produces a fusion pore that is lined by polar lipid head groups, with their hydrophobic tails being in contact with the hydrophobic transmembrane domains. To achieve such an arrangement, the bilayer structure has to be disrupted. The arrangement of Fig. 4*B* should be considered a schematic illustration of such a structure but should not be viewed as a precise molecular picture.

When fusion pores are formed by SNAP-25Δ9 instead of wtSNAP-25, they exhibit lower conductance, suggesting a decrease in fusion pore diameter or an increase in fusion pore length. With SNAP-25Δ9, the C terminus of the four-helical bundle will be zipped less tightly, which should lead to a longer fusion pore as indicated in Fig. 4*C*, consistent with the observed lower fusion pore conductance and reduced rate of catecholamine release. The experiments described here were performed by introducing SNAP-25Δ9 via viral infection in bovine chromaffin cells that are not devoid of wild-type SNAP-25. SNARE-mediated fusion pores are presumably formed by multiple SNARE proteins, but it is unknown by how many (31). We thus cannot exclude the possibility that the observed changes reflect mixed fusion pores involving SNAP-25Δ9 as well as wtSNAP-25. Mixed fusion pores are also suggested by the requirement of much higher intracellular Ca^{2+} concentrations for stimulation of exocytosis in SNAP-25Δ9-expressing SNAP-25 knockout cells devoid of wtSNAP25 (12) compared with experiments with expression of SNAP-25Δ9 in wild-type cells (10). Nevertheless, the participation of SNAP-25Δ9 mutants in fusion pore formation is clearly evident from the observed changes in fusion pore properties as well as the parallel effects of either cleaving endogenous SNAP-25 with botulinum neurotoxin A (32) or expressing SNAP-25Δ9 in bovine chromaffin cells (10).

SNAP-25 knockout chromaffin cells exhibit a reduction in amperometric spike frequency to ≈30% compared with control cells, and the remaining events have significantly reduced amperometric foot signal duration. It has been suggested that these exocytotic events may not require the assembly of the SNARE complex or may (more likely) use alternative SNARE homologues (33). Fusion pores supported by this unidentified SNAP-25 homologue exhibit shorter fusion pore lifetime consistent with a role of SNAP-25 in determining the properties of the fusion pore.

In a recent study introducing linkers of increasing length between the synaptobrevin transmembrane domain and its SNARE domain, a progressive decrease in foot current amplitude and increase in foot duration was found (34) that is parallel to the changes in fusion pore properties described here for the SNAP-25Δ9 mutant. These linkers also increased the average amperometric spike half-width (34) as does the SNAP-25Δ9 mutant. Although it is possible that the kinetics of rapid release during the amperometric spike is determined by an expanding fusion pore, it is also possible that the release kinetics reflects dissociation from the granular matrix (35). Strong support for the latter mechanism has come from the recent observation that the amperometric spike half-width is decreased in chromaffin cells lacking Chromogranin A (36). Our results clearly indicate that release, even at this late stage, is accelerated by molecular pulling of the SNAREs, either by affecting an expanded fusion pore or by exerting forces on the granule affecting the dissociation kinetics from its matrix.

Fusion pore dynamics is affected by intracellular Ca^{2+} concentrations (22–25) as well as overexpression of different synaptotagmin isoforms or synaptotagmin mutants (25–27). Although it is possible that synaptotagmin affects the fusion pore mechanics directly, it is also possible that the final zipping of the SNARE complex is not producing a unique structure but might depend on specific Ca^{2+}/synaptotagmin action, leading to variability in the conformation of SNARE complexes that lead to fusion. The nonexponential fusion pore lifetime distributions (Fig. 2 *C* and *D*) support such heterogeneity.

In the sequence of steps involved in vesicle fusion (Fig. 4*D*, solid line) the transition from the primed state to the fully zipped state is triggered by Ca^{2+} via a mechanism involving synaptotagmin and complexin (37). Because of the links of the SNARE domains to the transmembrane domains of synaptobrevin and syntaxin and their interactions with the membranes, the tension exerted by this fully zipped complex relaxes via opening of the fusion pore. For the SNAP-25Δ9 mutant, the SNARE complex is zipped less tightly and exerts less tension on the membranes, thus corresponding to a more relaxed lower energy state (Fig. 4*D*, dashed line). There is thus a lower probability from this state to proceed to the opening of the fusion pore, as is reflected in the smaller amplitude and slower kinetics of the exocytotic burst in cells expressing the SNAP-25Δ9 mutant (10). The narrow fusion pore state (Fig. 4*B*) is still characterized by significant tension and eventually relaxes by fusion pore expansion. For fusion pores involving SNAP-25Δ9, the tension in this state will again be lower, explaining the decreased fusion pore expansion rate. The changes in fusion pore properties in exocytosis medi-

ated by the SNAP-25Δ9 mutant are thus consistent with a model for fusion pore mechanics that couple N- to C-terminal zipping of the SNARE complex to opening of a fusion pore formed by a proteolipid complex of molecular dimensions.

Experimental Procedures

Cell Preparation and Protein Expression. Bovine chromaffin cells were prepared as described (38). Cells were incubated at 37°C and 10% CO_2 and infected at day 1–2 after isolation, and the cells were used 24–36 h after infection. Virus production and infection was performed as described (39). cDNAs encoding for N-terminally GFP-linked GFP-SNAP-25A and GFP-SNAP-25Δ9 were subcloned into the viral plasmid pSFV1 (Invitrogen). Plasmid sequences were confirmed by DNA sequencing.

Electrophysiology. Cell-attached patch-clamp capacitance measurements were performed with wide-tipped patch pipettes (tip diameter 5–7 μm) using an EPC-7 amplifier (HEKA) and a lock-in amplifier (SR 830; Stanford Research Systems) using a 20-kHz, 50-mV (root-mean square) sine wave and fusion pore conductances analyzed as described (19). Analysis of fusion pore conductance was restricted to fusion pores with lifetimes >15 ms because shorter events were distorted by the lock-in amplifier low-pass filter (set to 1 ms, 24 dB). The bath solution contained 140 mM NaCl, 5 mM KCl, 5 mM $CaCl_2$, 1 mM $MgCl_2$, 10 mM Hepes/NaOH, and 20 mM glucose (pH 7.3). The pipette solution contained 50 mM NaCl, 100 mM TEA-Cl, 5 mM KCl, 5 mM $CaCl_2$, 1 mM $MgCl_2$, and 10 mM Hepes/NaOH (pH 7.3). All experiments were done at room temperature.

Amperometry. Carbon fiber electrodes with a diameter of 5 μm (ALA Scientific Instruments) were used for amperometric measurements. Amperometric currents were recorded with an EPC-7 amplifier (HEKA) applying electrode voltage +700 mV, filtered at 3 kHz and analyzed by a customized macro for IGOR software (40). The analysis was restricted to events with a peak amplitude >10 pA. For foot-signal analysis, the amperometric currents were subsequently filtered with a 100-Hz digital Bessel filter and 60-Hz notch (IGOR IFDL; WaveMetrics), and analysis was restricted to events with foot current >0.5 pA and foot duration >4 ms. The bath solution contained 140 mM NaCl, 5 mM KCl, 5 mM $CaCl_2$, 1 mM $MgCl_2$, 10 mM Hepes/NaOH, 20 mM glucose (pH 7.3). Release events were stimulated by applications of high KCl solution: 30 mM NaCl, 100 mM KCl, 5 mM $CaCl_2$, 1 mM $MgCl_2$, 20 mM Glucose, and 10 mM Hepes-NaOH (pH 7.3) for 5 min.

ACKNOWLEDGMENTS. We thank Owasco Meat Co., Moravia, NY, for providing bovine adrenal glands, Joan Lenz for excellent technical assistance, Drs. Eugene Mosharov and David Sulzer for the Igor macro used for amperometric data analysis, Dr. Jens Rettig, who generously provided the SNAP-25Δ9 construct, and Dr. Erwin Neher for his support in all our experiments with the SNAP-25Δ9 from the beginning to invaluable discussions and critical comments on the manuscript. This work was supported by National Institutes of Health Grant R01-NS38200 and by the Nanobiotechnology Center (a Science and Technology Centers program of National Science Foundation Agreement No. ECS9876771).

1. Breckenridge LJ, Almers W (1987) Currents through the fusion pore that forms during exocytosis of a secretory vesicle. *Nature* 328:814–817.
2. Lindau M, Alvarez de Toledo G (2003) The fusion pore. *Biochim Biophys Acta* 1641:167–173.
3. Jahn R, Lang T, Sudhof TC (2003) Membrane fusion. *Cell* 112:519–533.
4. Almers W, Tse FW (1990) Transmitter release from synapses: Does a preassembled fusion pore initiate exocytosis? *Neuron* 4:813–818.
5. Han X, Wang CT, Bai J, Chapman ER, Jackson MB (2004) Transmembrane segments of syntaxin line the fusion pore of Ca2+-triggered exocytosis. *Science* 304:289–292.
6. Han X, Jackson MB (2005) Electrostatic interactions between the syntaxin membrane anchor and neurotransmitter passing through the fusion pore. *Biophys J* 88:L20–L22.
7. Chernomordik LV, Kozlov MM (2005) Membrane hemifusion: crossing a chasm in two leaps. *Cell* 123:375–382.
8. Wong JL, Koppel DE, Cowan AE, Wessel GM (2007) Membrane hemifusion is a stable intermediate of exocytosis. *Dev Cell* 12:653–659.
9. Sutton RB, Fasshauer D, Jahn R, Brunger AT (1998) Crystal structure of a SNARE complex involved in synaptic exocytosis at 2.4 Å resolution. *Nature* 395:347–353.
10. Wei S, *et al.* (2000) Exocytotic mechanism studied by truncated and zero layer mutants of the C-terminus of SNAP-25. *EMBO J* 19:1279–1289.
11. Criado M, Gil A, Viniegra S, Gutierrez LM (1999) A single amino acid near the C terminus of the synaptosome associated protein of 25 kDa (SNAP-25) is essential for exocytosis in chromaffin cells. *Proc Natl Acad Sci USA* 96:7256–7261.
12. Sorensen JB, *et al.* (2006) Sequential N- to C-terminal SNARE complex assembly drives priming and fusion of secretory vesicles. *EMBO J* 25:955–966.
13. Chow RH, Rüden Lv, Neher E (1992) Delay in vesicle fusion revealed by electrochemical monitoring of single secretory events in adrenal chromaffin cells. *Nature* 356:60–63.
14. Albillos A, *et al.* (1997) The exocytotic event in chromaffin cells revealed by patch amperometry. *Nature* 389:509–512.
15. Dernick G, Alvarez de Toledo G, Lindau M (2003) Exocytosis of single chromaffin granules in cell-free inside-out membrane patches. *Nat Cell Biol* 5:358–362.
16. Gong LW, de Toledo GA, Lindau M (2007) Exocytotic catecholamine release is not associated with cation flux through channels in the vesicle membrane but Na(+) influx through the fusion pore. *Nat Cell Biol* 9:915–922.
17. Neher E, Marty A (1982) Discrete changes of cell membrane capacitance observed under conditions of enhanced secretion in bovine adrenal chromaffin cells. *Proc Natl Acad Sci USA* 79:6712–6716.
18. Lollike K, Borregaard N, Lindau M (1995) The exocytotic fusion pore of small granules has a conductance similar to an ion channel. *J Cell Biol* 129:99–104.
19. Debus K, Lindau M (2000) Resolution of patch capacitance recordings and of fusion pore conductances in small vesicles. *Biophys J* 78:2983–2997.
20. Lollike K, Borregaard N, Lindau M (1998) Capacitance flickers and ''pseudoflickers'' of small granules, measured in the cell attached configuration. *Biophys J* 75:53–59.
21. Alés E, *et al.* (1999) High calcium concentrations shift the mode of exocytosis to the kiss-and-run mechanism. *Nat Cell Biol* 1:40–44.
22. Hartmann J, Lindau M (1995) A novel Ca^{2+}-dependent step in exocytosis subsequent to vesicle fusion. *FEBS Lett* 363:217–220.
23. Fernández-Chacón R, Alvarez de Toledo G (1995) Cytosolic calcium facilitates release of secretory products after exocytotic vesicle fusion. *FEBS Lett* 363:221–225.
24. Scepek S, Coorssen JR, Lindau M (1998) Fusion pore expansion in horse eosinophils is modulated by Ca^{2+} and protein kinase C via distinct mechanisms. *EMBO J* 17:4340–4345.
25. Wang CT, Bai J, Chang PY, Chapman ER, Jackson MB (2006) Synaptotagmin-Ca2+ triggers two sequential steps in regulated exocytosis in rat PC12 cells: Fusion pore opening and fusion pore dilation. *J Physiol* 570:295–307.
26. Wang CT, *et al.* (2001) Synaptotagmin modulation of fusion pore kinetics in regulated exocytosis of dense-core vesicles. *Science* 294:1111–1115.
27. Bai J, Wang CT, Richards DA, Jackson MB, Chapman ER (2004) Fusion pore dynamics are regulated by synaptotagmin*t-SNARE interactions. *Neuron* 41:929–942.
28. Austin RH, Beeson KW, Eisenstein L, Frauenfelder H, Gunsalus IC (1975) Dynamics of ligand binding to myoglobin. *Biochemistry* 14:5355–5373.
29. Lindau M, Rüppel H (1983) Evidence for conformational substates of rhodopsin from kinetics of light-induced charge displacement. *Photobiochem Photobiophys* 5:219–228.
30. Takamori S, *et al.* (2006) Molecular anatomy of a trafficking organelle. *Cell* 127:831–846.
31. Montecucco C, Schiavo G, Pantano S (2005) SNARE complexes and neuroexocytosis: How many, how close? *Trends Biochem Sci* 30:367–372.
32. Xu T, Binz T, Niemann H, Neher E (1998) Multiple kinetic components of exocytosis distinguished by neurotoxin sensitivity. *Nat Neurosci* 1:192–200.
33. Sorensen JB, *et al.* (2003) Differential control of the releasable vesicle pools by SNAP-25 splice variants and SNAP-23. *Cell* 114:75–86.
34. Kesavan J, Borisovska M, Bruns D (2007) v-SNARE actions during Ca(2+)-triggered exocytosis. *Cell* 131:351–363.
35. Wightman RM, Troyer KP, Mundorf ML, Catahan R (2002) The association of vesicular contents and its effects on release. *Ann NY Acad Sci* 971:620–626.
36. Montesinos MS, *et al.* (2008) The crucial role of chromogranins in storage and exocytosis revealed using chromaffin cells from chromogranin A null mouse. *J Neurosci* 28:3350–3358.
37. Tang J, *et al.* (2006) A complexin/synaptotagmin 1 switch controls fast synaptic vesicle exocytosis. *Cell* 126:1175–1187.
38. Parsons TD, Coorssen JR, Horstmann H, Almers W (1995) Docked granules, the exocytic burst, and the need for ATP hydrolysis in endocrine cells. *Neuron* 15:1085–1096.
39. Ashery U, Betz A, Xu T, Brose N, Rettig J (1999) An efficient method for infection of adrenal chromaffin cells using the Semliki Forest virus gene expression system. *Eur J Cell Biol* 78:525–532.
40. Mosharov EV, Sulzer D (2005) Analysis of exocytotic events recorded by amperometry. *Nat Methods* 2:651–658.